THEORETICAL ANALYSIS OF PULSE AND DIFFERENTIAL PULSE POLAROGRAPHY OF REVERSIBLE REDOX REACTION COMPLICATED BY REACTANT ADSORPTION

Milivoj LOVRIĆ*, MARINA ZELIĆ[1] and Šebojka KOMORSKY-LOVRIĆ[2]

Center for Marine Research, "Ruđer Bošković" Institute, POB 180, 10002 Zagreb, Croatia; e-mail: [1] zelic@rudjer.irb.hr, [2] slovric@rudjer.irb.hr

Received November 6, 2000
Accepted January 2, 2001

Presented at the J. Heyrovský Memorial Symposium, Prague, August 30–September 1, 2000.

Pulse and differential pulse polarograms of redox reactions complicated by reactant adsorption with and without lateral attractions in the monolayer are analysed theoretically by using a stationary spherical diffusion model. The continuous shift of the post-peak potential to lower values and the decrease in its half-peak width with increasing bulk concentration of reactant indicate attractions between adsorbed ions or molecules.

Keywords: Pulse polarography; Differential pulse polarography; Stationary spherical diffusion model; Adsorption; Static mercury drop electrode; $PbBr_2$.

The dc polarogram of a reversible redox reaction complicated by reactant adsorption on the surface of static mercury drop electrode often consists of a main wave and a post-wave separated by a minimum[1–3]. This phenomenon was observed in experiments with lead ions in bromide medium[1]. It is caused by the adsorption of neutral complex $PbBr_2$ followed by the surface complexation mechanism: $x\ PbBr_2 + (Br^-)_{ads} \rightleftarrows (PbBr_2)_xBr^-)_{ads}$, where $x \leq 5$ (ref.[2]). The minimum separating diffusion and adsorption waves was analysed for Langmuir and Frumkin isotherms[3]. It was shown that the minimum followed by a steep post-wave is the indication of strong lateral attractions in the adsorbed layer. In the present communication, the influence of attractions on pulse and differential pulse polarograms of the surface redox reaction is investigated. The sensitivity of these two techniques to adsorbed reactants is well known[4–10].

THEORETICAL

A reversible redox reaction complicated by adsorption of reactant on the surface of the static mercury drop electrode is considered.

$$(\mathrm{Ox})_{\mathrm{ads}} \rightleftarrows \mathrm{Ox} + n\,\mathrm{e} \rightleftarrows \mathrm{Red}\,. \qquad (1)$$

The mass transfer is described by the spherical diffusion model:

$$\partial(rc_{\mathrm{ox}})/\partial t = D\,\partial^2(rc_{\mathrm{ox}})/\partial r^2\,, \qquad (2)$$

$$\partial(rc_{\mathrm{red}})/\partial t = D\,\partial^2(rc_{\mathrm{red}})/\partial r^2\,, \qquad (3)$$

$$t = 0, r \geq r_0\colon \quad c_{\mathrm{ox}} = c_{\mathrm{ox}}^*\,, c_{\mathrm{red}} = 0, \Gamma_{\mathrm{ox}} = 0\,, \qquad (4)$$

$$t > 0, r \to \infty\colon \quad c_{\mathrm{ox}} \to c_{\mathrm{ox}}^*\,, c_{\mathrm{red}} \to 0 \qquad (5)$$

$$r = r_0\colon \quad (c_{\mathrm{ox}})_{r=r_0} = (c_{\mathrm{red}})_{r=r_0} \exp(\varphi) \qquad (6)$$

$$\varphi = nF(E - E^0)/RT \qquad (7)$$

$$D(\partial c_{\mathrm{ox}}/\partial r)_{r=r_0} = I/nFS + \mathrm{d}\Gamma_{\mathrm{ox}}/\mathrm{d}t \qquad (8)$$

$$D(\partial c_{\mathrm{red}}/\partial r)_{r=r_0} = -I/nFS \qquad (9)$$

$$\beta(c_{\mathrm{ox}})_{r=r_0} = \theta \exp(a\theta)/(1-\theta)\,, \qquad (10)$$

where: $\theta = \Gamma_{ox} / \Gamma_{max}$ and Γ_{max} is the maximum surface concentration of the adsorbed reactant, r and t are space and time coordinates, r_0 is the radius of the static mercury drop electrode, c_{ox} and c_{red} are concentrations of the reactant and the product, respectively, c^*_{ox} is the bulk concentration of the reactant, $(c_{ox})_{r=r_0}$ and $(c_{red})_{r=r_0}$ are concentrations of the reactant and product at the electrode surface, respectively, D is a diffusion coefficient, E is electrode potential, E^0 is the standard potential of the simple redox reaction $Ox + ne \rightleftarrows Red$, F is the Faraday constant, I is the current, n is the number of electrons, R is the gas constant, S is the electrode surface area, β is adsorption constant of the reactant, Γ_{ox} is surface concentration of the adsorbed reactant and a is Frumkin coefficient of the reactant. A negative value of the Frumkin coefficient ($a < 0$) corresponds to intermolecular attraction between adsorbed molecules.

Equations (*2*) and (*3*) can be solved by the substitution $\Psi = c_{ox} + c_{red}$ (ref.[1]). The application of Laplace transforms and the modified Nicholson and Olmstead methods yields a system of recursive formulae for the degree of coverage of electrode surface

$$(\theta_m - 1)(\theta_m - \omega_m) = y\,\theta_m \exp(a\theta_m)\,, \qquad (11)$$

where θ_m is the surface coverage at $t = md$ and d is the time increment, $m = 1, 2 \ldots M$, $M = t_d/d$ and t_d is a mercury drop life-time. The meanings of the other symbols are the following

$$\omega_m = b^2(\pi M Q_1 \gamma)^{-1} - Q_1^{-1} \sum_{j=1}^{m-1} \theta_j (Q_{m-j+1} - Q_{m-j})\,, \qquad (12)$$

$$y = b^2[1 + \exp(-\varphi)](\pi M Q_1 z)^{-1}\,, \qquad (13)$$

$$b = (\pi t_d D)^{1/2} / r_0\,, \qquad (14)$$

$$z = \beta\Gamma_{max} / r_0\,, \qquad (15)$$

$$\gamma = \Gamma_{max} / c^*_{ox} r_0 , \tag{16}$$

$$\begin{aligned} Q_k &= \exp[b^2 (k-1)(\pi M)^{-1}] \operatorname{erfc}[b(k-1)^{1/2} (\pi M)^{-1/2}] - \\ &- \exp[b^2 k(\pi M)^{-1}] \operatorname{erfc}[bk^{1/2} (\pi M)^{-1/2}]. \end{aligned} \tag{17}$$

The integral equations for the currents immediately before and at the end of the pulse can be obtained by solving Eq. (*3*)

$$\begin{aligned} \Phi_i &= \{(2M^{1/2} + b)[(c_{red})_{r=r_0} / c^*_{ox}]_i + \\ &+ 2M^{1/2} \sum_{j=1}^{i-1} [(c_{red})_{r=r_0} / c^*_{ox}]_j (P_{i-j+1} - P_{i-j})\} (M - M_0)^{1/2} M^{-1/2} / (1+b), \end{aligned} \tag{18}$$

where either $i = M_0$, or $i = M$, $t_P = (M - M_0)d$ and t_P is a pulse duration time. The meanings of other symbols are the following

$$[(c_{red})_{r=r_0} / c^*_{ox}]_m = \theta_m \gamma (1-\theta_m)^{-1} z^{-1} \exp(-\varphi + a\theta_m) , \tag{19}$$

$$\Phi = I(\pi t_p)^{1/2} (nFSc^*_{ox})^{-1} D^{-1/2} (1+b)^{-1}, \tag{20}$$

$$P_k = k^{1/2} - (k-1)^{1/2} . \tag{21}$$

The pulse and differential pulse polarography were simulated using M = 500 and M_0 = 475 which ensured optimum speed and precision of the simulation[3].

RESULTS AND DISCUSSION

The parameter γ is inversely proportional to the relative bulk concentration of the reactant. It determines the relationship between the main peak and the post-peak in differential pulse polarography (DPP) as can be seen in Fig. 1. The main peak is well developed if $\gamma < 0.06$ (see curves *1–3*). If $\Gamma_{max} = 5 \cdot 10^{-10}$ mol/cm^2 and r_0 = 0.03 cm, this value of γ corresponds to $c^*_{ox} > 3 \cdot 10^{-4}$ mol/l. This figure also shows that the dimensionless post-peak is twice higher than the main peak (*cf.* curves *1* and *7*). Hence, the sensitivity of DPP, *i.e.* the gradient $\partial I / \partial c^*_{ox}$, is higher for the adsorbed reactant ($\gamma > 1$)

than for the dissolved reactant ($\gamma < 10^{-2}$). Besides, the half-peak widths of the main peak and the post-peak are 100 and 70 mV, respectively, both for the pulse amplitude of 50 mV. In the absence of interactions between adsorbed molecules ($a = 0$), the separation between two peaks depends linearly on logarithm of the dimensionless adsorption constant

$$E_{P,1} - E_{P,2} = 0.058(1 + \log z) \,. \qquad (22)$$

This is shown in Fig. 2. However, for very weak adsorption ($z = 1$), these two peaks are unresolved. Figure 3 shows that in this case the variation of the reactant bulk concentration causes the shift of the peak potential for 60 mV (see also curve *1* in Fig. 4). If $r_0 = 0.03$ cm, the value $z = 1$ corresponds to the product $\beta\Gamma_{max} = 3 \cdot 10^{-2}$ cm. This product is the adsorption constant of a linear isotherm. For many surface-active ions and organic substances the value of this constant is between 10^{-2} and 1 cm (refs[2,4,7]). Hence, the adsorption characterized by $z = 10$ and $a = 0$ is moderately strong (see Fig. 1). Curve *3* in Fig. 4 shows the relationship between DPP peak potentials and the reactant concentration for this case. A small shift of the post-peak in the positive direction appears in the range of the smallest relative concentrations. A similar shift can be observed on curve *1* of this figure. With the development of the main peak at +0.025 V *vs* E^0, the post-peak shifts nega-

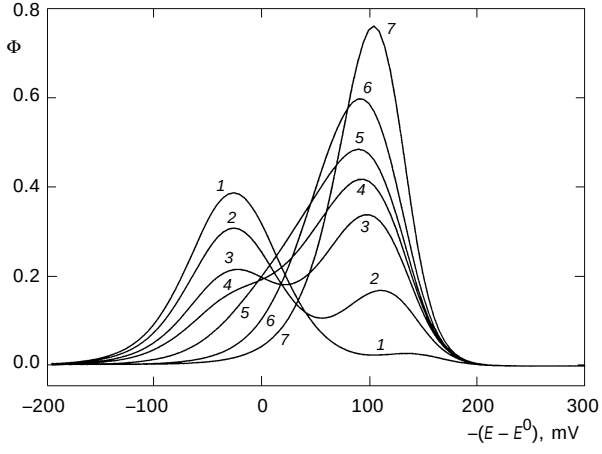

FIG. 1
Differential pulse polarograms of the redox reaction (Eq. (*1*)): $\Delta E = 50$ mV, $n = 1$, $t_p/t_d = 0.05$, $b = 0.1$, $a = 0$, $z = 10$ and $\gamma = 0.01$ (*1*), 0.03 (*2*), 0.05 (*3*), 0.06 (*4*), 0.07 (*5*), 0.1 (*6*) and 1 (*7*)

tively. For this reason Eq. (*22*) applies only to polarograms with two approximately equal peaks, such as those shown in Fig. 2. In all other cases, the difference is by 10–40 mV bigger, depending on $1/\gamma$.

Under the influence of lateral attractions in the adsorbed layer, the separation between the diffusion and adsorption peaks increases, while the

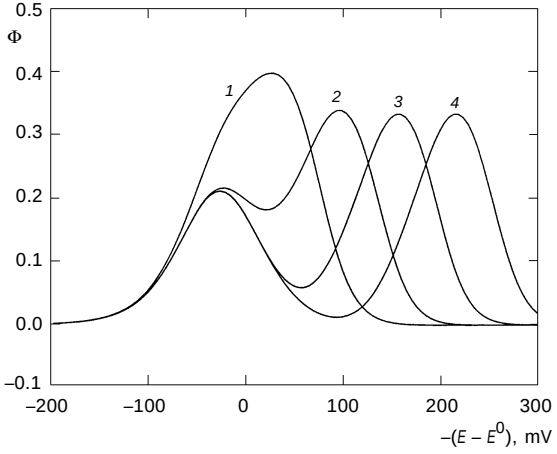

FIG. 2
Differential pulse polarograms of the redox reaction (Eq. (*1*)): $\gamma = 0.05$ and $z = 1$ (*1*), 10 (*2*), 100 (*3*) and 1 000 (*4*). For other parameters, see Fig. 1

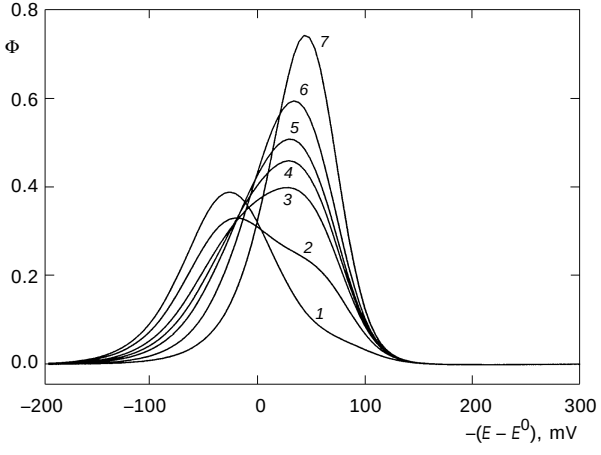

FIG. 3
Differential pulse polarograms of the redox reaction (Eq. (*1*)): $z = 1$ and $\gamma = 0.01$ (*1*), 0.03 (*2*), 0.05 (*3*), 0.06 (*4*), 0.07 (*5*), 0.1 (*6*) and 1 (*7*). For other parameters, see Fig. 1

half-peak width of the post-peak decreases to 60 mV for $a = -2$, 40 mV for $a = -3$ and 20 mV for $a = -4$. This can be seen in Fig. 5. The difference between peak potentials is directly proportional to the Frumkin coefficient a, with the slope $\partial(E_{P,1} - E_{P,2})/\partial a = -15$ mV (note that $a < 0$). The influences of the

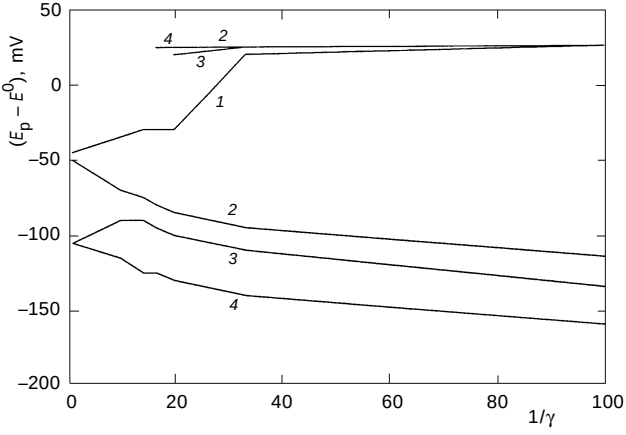

FIG. 4
Dependence of peak potentials of differential pulse polarograms of the redox reaction (Eq. (*1*)) on the relative bulk concentration of the reactant: $z = 1$, $a = 0$ (*1*); $z = 1$, $a = -3$ (*2*); $z = 10$, $a = 0$ (*3*); $z = 10$, $a = -2$ (*4*). For other parameters, see Fig. 1

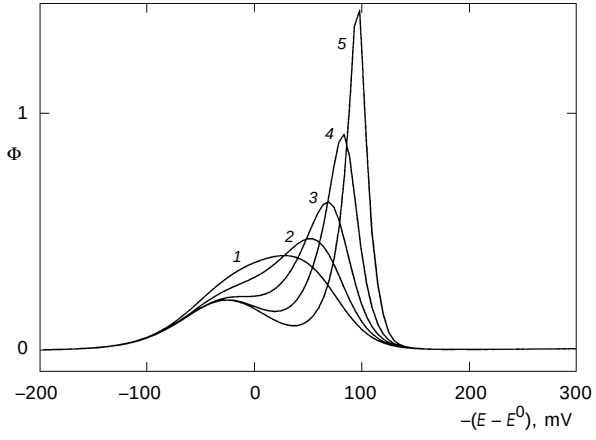

FIG. 5
Differential pulse polarograms of the redox reaction (Eq. (*1*)): $z = 1$, $\gamma = 0.05$ and $a = 0$ (*1*), –1 (*2*), –2 (*3*), –3 (*4*) and –4 (*5*). For other parameters, see Fig. 1

Frumkin coefficient and the dimensionless adsorption constant are simply additive

$$E_{P,1} - E_{P,2} = 0.058(1 + \log z) - 0.015a \ . \qquad (23)$$

Equation (*23*) applies under the same conditions as Eq. (*22*).

Figure 6 shows that the attraction forces influence DPP polarograms only in the concentration range in which the main peak develops. Curve *7* is almost identical with curve *7* in Fig. 3. They appear at low surface coverage. As the relative bulk concentration of the reactant increases, the post-peak shifts in negative direction, its half-peak width decreases and a main peak appears. Under these conditions, the electrode surface is fully covered by the adsorbed reactant before application of the pulse and the post-peak corresponds to the reduction of condensed rectant monolayer. The peak potentials of polarograms in Fig. 6 are plotted as curve *2* in Fig. 4. Curve *4* in Fig. 4 shows peak potentials influenced by stronger adsorption, but weaker attraction (z = 10, a = –2). Curves *2* and *4* are to be compared with curves *1* and *3*, respectively. The differences among them are the most significant in the range of the lowest concentrations ($1/\gamma < 20$), where the respective curves diverge. Hence, the continuous shift of the post-peak in negative direction, together with the decrease of the half-peak width below 70 mV, are

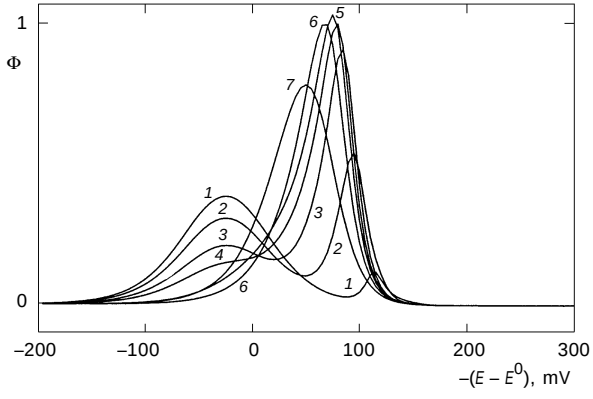

FIG. 6
Differential pulse polarograms of the redox reaction (Eq. (*1*)): z = 1, a = –3 and γ = 0.01 (*1*), 0.03 (*2*), 0.05 (*3*), 0.06 (*4*), 0.07 (*5*), 0.1 (*6*) and 1 (*7*). For other parameters, see Fig. 1

the indications of lateral attractions in the adsorbed layer. The effect is more pronounced if the adsorption constant is lower, but the attraction forces are stronger.

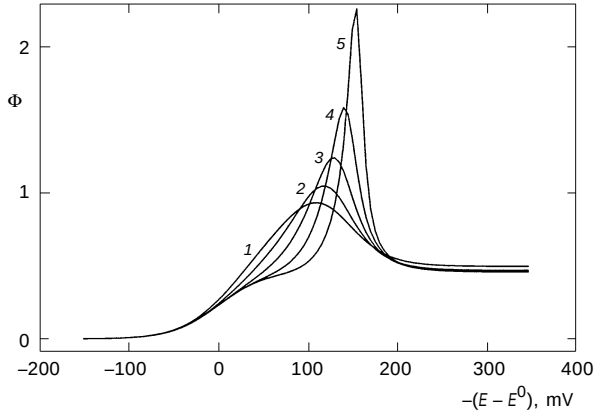

FIG. 7
Pulse polarograms of the redox reaction (Eq. (*1*)): t_P/t_d = 0.05, b = 0.1, n = 1, z = 1, γ = 0.05 and a = 0 (*1*), –1 (*2*), –2 (*3*), –3 (*4*) and –4 (*5*)

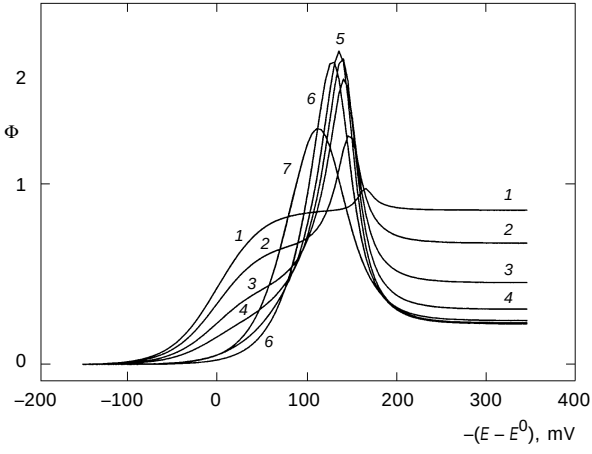

FIG. 8
Pulse polarograms of the redox reaction (Eq. (*1*)): z = 1, a = –3 and γ = 0.01 (*1*), 0.03 (*2*), 0.05 (*3*), 0.06 (*4*), 0.07 (*5*), 0.1 (*6*) and 1 (*7*). For other parameters, see Fig. 7

Figure 7 shows the influence of the Frumkin parameter a on the pulse polarogram of the redox reaction (*1*). The separation between the half-wave potential of diffusion wave and the potential of adsorption peak depends linearly on the interaction parameter and the logarithm of dimensionless adsorption constant

$$E_{1/2} - E_p = 0.110 + 0.058 \log z - 0.012a \, . \qquad (24)$$

The half-peak width decreases from 100 mV for $a = 0$ to 80 mV ($a = -1$), 60 mV ($a = -2$), 40 mV ($a = -3$) and 25 mV ($a = -4$). The dimensionless peak current is independent of the adsorption constant, but increases with the Frumkin parameter.

The dependence of pulse polarograms on the concentration parameter γ is shown in Fig. 8. The development of the main wave is accompanied by the shift of adsorption peak in negative direction, like in DPP. The relationship between the peak potentials and the relative bulk concentration of the reactant is presented as the curve *1* in Fig. 9. Curves *2* and *3* of this figure show the same relations corresponding to the stronger adsorption without and with attractions, respectively. The similarity of Figs 4 and 9 shows that the manifestations of attraction are the same in both pulse and differential

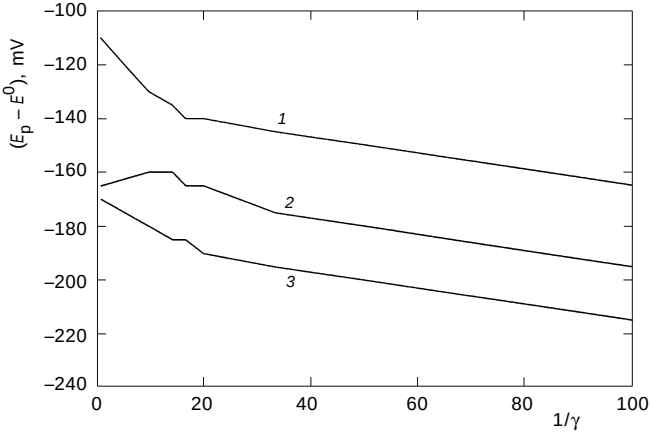

FIG. 9

Dependence of peak potentials of pulse polarograms of the redox reaction (Eq. (*1*)) on the relative bulk concentration of the reactant: $z = 1$, $a = -3$ (*1*); $z = 10$, $a = 0$ (*2*); $z = 10$, $a = -2$ (*3*). For other parameters, see Fig. 7

pulse polarography. It is very probable that many polarograms consisting of a clearly separated main peak and post-peak are caused by weak adsorption enhanced by lateral attractions in the monolayer, rather than by strong adsorption alone.

REFERENCES

1. Zelić M., Lovrić M.: *Electrochim. Acta* **1990**, *35*, 1701.
2. Lovrić M., Komorsky-Lovrić Š.: *Langmuir* **1995**, *11*, 1784.
3. Lovrić M.: *J. Electroanal. Chem.* **1999**, *465*, 30.
4. van Leeuwen H. P., Buffle J., Lovrić M.: *Pure Appl. Chem.* **1992**, *64*, 1015.
5. Lovrić M., Zelić M.: *J. Electroanal. Chem.* **1991**, *316*, 315.
6. Puy J., Mas F., Diaz-Cruz J. M., Esteban M., Casassas E.: *Anal. Chim. Acta* **1992**, *268*, 261.
7. Fatouros N., Krulic D.: *J. Electroanal. Chem.* **1999**, *478*, 25.
8. Lovrić M.: *J. Electroanal. Chem.* **1987**, *218*, 77.
9. Pižeta I., Lovrić M., Zelić M., Branica M.: *J. Electroanal. Chem. Interfacial Electrochem.* **1991**, *318*, 25.
10. Zelić M., Pižeta I., Branica M.: *Anal. Chim. Acta* **1993**, *281*, 63.